



Contents lists available at ScienceDirect

## Bioorganic &amp; Medicinal Chemistry

journal homepage: [www.elsevier.com/locate/bmc](http://www.elsevier.com/locate/bmc)

## Discovery of a novel chimeric ubenimex–gemcitabine with potent oral antitumor activity

Yuqi Jiang<sup>a</sup>, Jinning Hou<sup>a</sup>, Xiaoyang Li<sup>a</sup>, Yongxue Huang<sup>b</sup>, Xuejian Wang<sup>c</sup>, Jingde Wu<sup>a</sup>, Jian Zhang<sup>c</sup>, Wenfang Xu<sup>a</sup>, Yingjie Zhang<sup>a,\*</sup>

<sup>a</sup> Department of Medicinal Chemistry, School of Pharmaceutical Sciences, Shandong University, 44 West Wenhua Road, 250012 Ji'nan, Shandong, PR China

<sup>b</sup> Weifang Bochuang International Biological Medicinal Institute, Weifang, Shandong 261061, PR China

<sup>c</sup> College of Pharmacy, Weifang Medical University, 261053 Weifang, Shandong, PR China

## ARTICLE INFO

## Article history:

Received 25 July 2016

Revised 12 September 2016

Accepted 13 September 2016

Available online xxxxx

## Keywords:

CD13 inhibitor

Ubenimex

Gemcitabine (GEM)

Anti-angiogenesis

Anticancer

## ABSTRACT

Herein, a novel mutual prodrug **BC-A1** was discovered by integrating ubenimex and gemcitabine into one molecule. Biological characterization revealed that compound **BC-A1** could maintain both the anti-CD13 activity of ubenimex and the cytotoxic activity of gemcitabine in vitro. Further characterization also demonstrated that compound **BC-A1** exhibited significant anti-invasion and anti-angiogenesis effects in vitro. The preliminary stability test of **BC-A1** revealed that it could release gemcitabine in vitro. The in vivo anti-tumor results in liver cancer showed that at the same dosage, oral administration of **BC-A1** was as potent as intraperitoneal administration of gemcitabine. This warranted the further research and development of the orally active prodrug **BC-A1** because gemcitabine can not be orally administrated in clinic.

© 2016 Elsevier Ltd. All rights reserved.

### 1. Introduction

Aminopeptidase N (APN/CD13), a membrane-bound metallo-protease widely expressed on diverse cell surfaces,<sup>1–3</sup> is universally regarded as a multifunctional protein which involved in cancer invasion, angiogenesis, metastasis peptides degradation and so on.<sup>2,4–6</sup> Moreover, CD13 has been described as a functional biomarker of angiogenesis and surface marker of semi-dormant liver cancer stem cells (CSCs) in human liver cancer cell lines.<sup>7–10</sup> Ubenimex (Bestatin, Ube, **1**), a natural product, is the only marketed inhibitor of CD13, which is used as immune enhancement for the treatment of leukemia or act as an adjuvant agent with other anti-cancer drugs.<sup>11–13</sup>

Gemcitabine (GEM), a nucleoside analogue, is widely used for treating a variety of solid tumors, such as non-small lung, pancreatic, breast, ovarian cancers and so on.<sup>14–22</sup> Gemcitabine was first launched in 1995 by Lilly.<sup>14</sup> After that, combination of gemcitabine and other cytotoxic antitumor agents or targeted drugs in cancer treatment are already in advanced clinical trials.<sup>23–26</sup> Although gemcitabine is widely used, the clinical use of gemcitabine is also subjected to some limitations, such as rapid metabolic inactivation, poor oral bioavailability, drug resistance, and so on.<sup>27–30</sup> After administration of gemcitabine, more than 90% of gemcitabine is

catalyzed by cytidine deaminase (CDA) and deoxycytidylate deaminase (DCD) and converted to its inactive metabolite, 2,2'-difluoro-deoxyuridine (dFdU) and its monophosphate derivative (dFdUMP).<sup>31,32</sup> In order to overcome most of the aforementioned problems, many gemcitabine derivatives were designed and synthesized via modifications of 4-(N)- and 5'-sites of gemcitabine (Fig. 1).<sup>33,34</sup> Among these compounds, LY2334737 is developed to improve the poor oral bioavailability of gemcitabine. LY2334737 is an oral gemcitabine prodrug, and in Phase I clinical trials.<sup>35</sup>

In our previous report, we presented the design and synthesis of a novel mutual prodrug **BC-O1** containing ubenimex and fluorouracil. Biological characterization of **BC-O1** proved that this novel mutual prodrug exhibited improved in vitro and in vivo antitumor efficiency and displayed multifunctional antitumor properties.<sup>36</sup> According to the similar mutual prodrug strategy, ubenimex and gemcitabine were directly integrated into one molecule to get compound **BC-A1** (Fig. 2), which was expected to be an orally active prodrug of ubenimex and gemcitabine. Besides, based on our previous results of **BC-O1**,<sup>36</sup> **BC-A1** itself should also possess CD13 inhibitory activity, possibly endowing **BC-A1** with tumor targeting property.

### 2. Chemistry

The compound **9** was synthesized starting from (3S,4R)-4-amino-3-hydroxy-2-oxo-5-phenylpentanoic acid (**10**, AHPA), as

\* Corresponding author. Tel.: +86 531 88382009.

E-mail address: [zhangyingjie@sdu.edu.cn](mailto:zhangyingjie@sdu.edu.cn) (Y. Zhang).

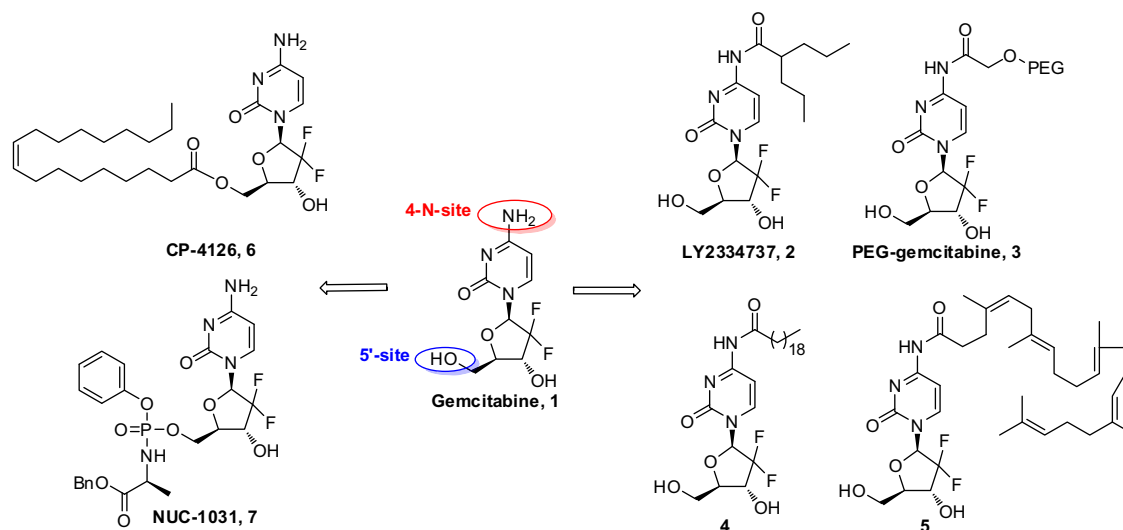


Figure 1. Structure of gemcitabine derivatives.

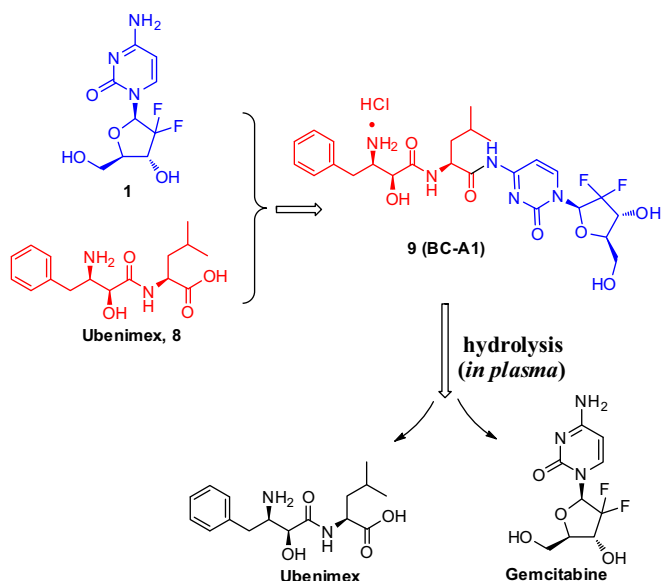


Figure 2. Design strategy, chemical structure and proposed degradation pathway of targeted compound.

illustrated in Scheme 1. Compound **10** was protected by the ditert-butyl dicarbonate (Boc group), followed by condensation with *L*-leucine give the compound **12**. Then deprotection of the benzyl group gave the free acid **13**. Gemcitabine hydrochloride (**14**) was protected by the silyl chloride (TBS group) to afford intermediate **15**, which was reacted with **13** in the presence 1-(3-dimethylaminopropyl)-3-ethylcarbodiimide hydrochloride (EDCI) and 1-hydroxybenzotriazole (HoBt) to afford the compound **16**. Deprotection of the TBS group gave the intermediate **17**. Treatment of **17** with hydrogen chloride (HCl) in acetic acid led to the target compound **9 (BC-A1)**.

### 3. Results and discussion

#### 3.1. In vitro CD13 inhibition

The  $IC_{50}$  ( $\mu M$ ) values of ubenimex and **BC-A1** toward CD13 from porcine kidney were determined to be 3.70 and 8.75  $\mu M$ , respectively (Table 1), which showed that the inhibitory activity

of **BC-A1** was slight weaker than the positive control ubenimex. Furthermore, we also assessed the inhibitory ability of **BC-A1** and ubenimex toward the human CD13, which is deriving from cultured A549 and PLC/PRF/5 cells. Similar to the above enzyme inhibitory activity, both **BC-A1** and ubenimex showed micromolar  $IC_{50}$  values (Table 1). These results confirmed that attachment of gemcitabine to the carboxyl group of ubenimex did not influence its binding ability to the active site of CD13, just like our previous reported mutual prodrug **BC-O1**.<sup>36</sup>

#### 3.2. Antiproliferative activity assay and colony-forming assay

11 kinds of solid or hematological tumor cell lines were selected to test the antiproliferative activity of **BC-A1**. Results (Table 2) showed that compared with its parent compound gemcitabine, **BC-A1** exhibited similar antiproliferative activity toward a broad range of cancer cell types including liver, lung, ovary, colon, breast and prostate cancer cells. However, the other parent compound of **BC-A1**, the CD13 inhibitor ubenimex exhibited no cytotoxicity. Moreover, the result in KG1 cell line shows that the combination of ubenimex and gemcitabine showed no synergistic effects. Collectively, these results indicated that **BC-A1** could release gemcitabine to exhibit antiproliferative activity. Additionally, cytotoxicity of **BC-A1** and gemcitabine against human liver cell HL-7702 was tested. The  $IC_{50}$  value of **BC-A1** and gemcitabine were 22.06  $\mu M$  and 5.43  $\mu M$ , respectively, which revealed the selectivity of **BC-A1** between nontransformed cells and tumor cells.

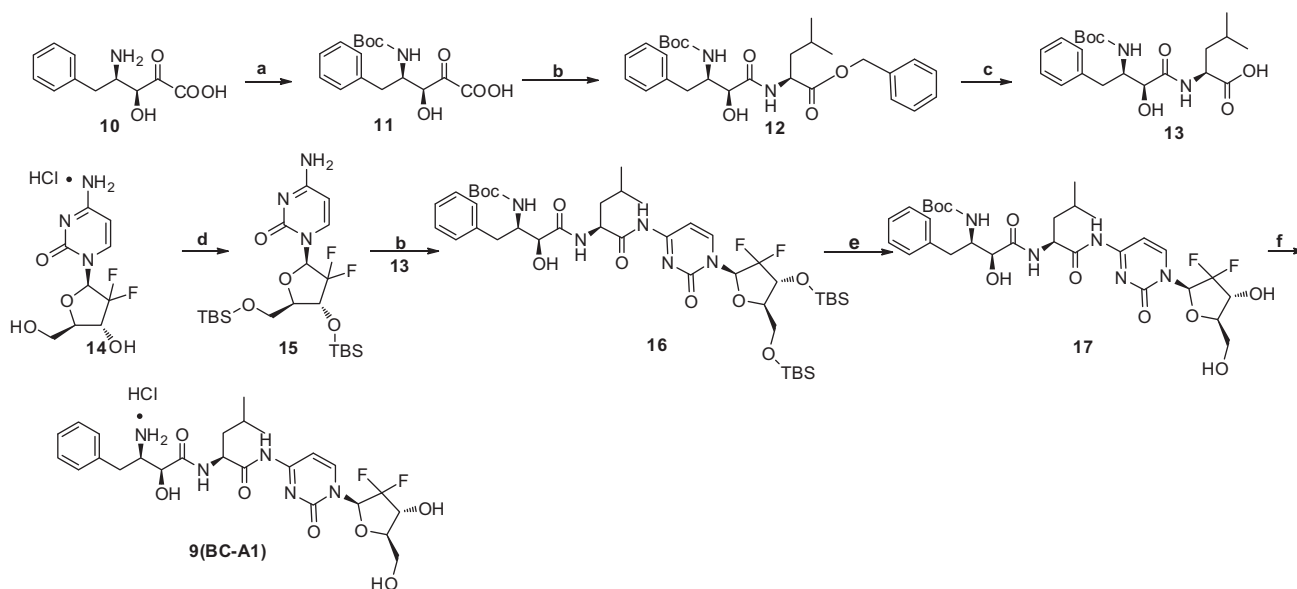
In order to further confirm the anti-proliferative activities of **BC-A1**, PLC/PRF/5 cell was chosen for the colony-forming assay. Similarly, the result demonstrated that **BC-A1** decreased the number of colonies formed (Fig. 3).

#### 3.3. Induction of apoptosis in vitro

Flow cytometry analysis was used to determine the effect of **BC-A1** in inducing apoptosis (Fig. 4). Results suggested that at the dose of 2  $\mu M$ , **BC-A1** could induce more tumor cells apoptosis than the positive control ubenimex, while displayed less potency than gemcitabine.

#### 3.4. Anti-invasion assay in vitro

Ubenimex could inhibit cancer-cell invasion in a dose-dependent manner, which has been shown to be attributed to inhibition



**Scheme 1.** Synthesis of compound **9**. (Reagents and conditions: (a)  $(\text{Boc})_2\text{O}$ , 1 N NaOH, THF; (b) EDCl, HoBt, DCM; (c) Pd/C,  $\text{H}_2$ , methanol; (d) *N*-methylimidazole, iodine, silyl chloride; (e) TBAF, THF and (f) dry HCl in EtOAc.)

**Table 1**  
CD13 inhibitory activity of **BC-A1** and ubenimex

Compd	$\text{IC}_{50}$ ( $\mu\text{M}$ ) <sup>a</sup> toward CD13 from porcine kidney	$\text{IC}_{50}$ ( $\mu\text{M}$ ) <sup>a</sup> toward CD13 on the surface of A549 cells	$\text{IC}_{50}$ ( $\mu\text{M}$ ) <sup>a</sup> toward CD13 on the surface of PLC/PRF/5 cells
<b>BC-A1</b>	$8.75 \pm 2.17$	$18.30 \pm 1.11$	$15.78 \pm 0.85$
Ubenimex	$3.70 \pm 1.06$	$17.34 \pm 0.10$	$40.65 \pm 9.41$

<sup>a</sup> Assays were performed in replicate ( $n \geq 2$ ); data are shown as mean  $\pm$  SD.

of CD13.<sup>37</sup> In order to examine the anti-invasion effect of the compound **BC-A1**, an anti-invasion assay was performed on transwell chambers coated with Matrigel. Treatment of ES-2 cells with **BC-A1** at 5  $\mu\text{g}/\text{mL}$  markedly decreased the invasion of cells through the matrigel basement membrane in comparison with the ubenimex and the negative control group (Fig. 5).

### 3.5. HUVEC tuber formation and rat thoracic aorta rings (TARs) assay

CD13 is a key target in anti-angiogenesis, and it was reported that ubenimex could inhibit the tubular structure formation of

HUVECs.<sup>38</sup> To investigate the anti-angiogenic effect of **BC-A1**, the in vitro HUVECs tube formation assays were performed. Treatment of HUVECs with compound **BC-A1** at 30  $\mu\text{M}$  within 8 h almost inhibited the tuber formation completely. Meanwhile **BC-A1** exhibited more tuber formation inhibitory activity than ubenimex at the same concentration (Fig. 6a).

Compared with HUVECs tuber formation model, rat thoracic aorta rings (TARs) assay is more close to in vivo condition in view of multi-steps involved in angiogenesis: sprouting, proliferation, migration and differentiation. Therefore, the anti-angiogenic activity of compound **BC-A1** was further evaluated in TARs assay. The results illustrated that at the concentration of 20  $\mu\text{g}/\text{mL}$ , **BC-A1** decreased the number of microvessels sprouting from aortic rings isolated from rat. Again, **BC-A1** showed better angiogenesis inhibitory activity than ubenimex at the same dosage (Fig. 6b).

### 3.6. The stability of **BC-A1** in human plasma

**BC-A1** is designed to be a targeted anticancer prodrug, so we need to evaluate the hydrolysis kinetics of **BC-A1** in plasma. To this end, HPLC method was developed to briefly study the cleavage of compound **BC-A1** in human plasma in vitro. We observed that

**Table 2**  
Antiproliferative activities of **BC-A1** against eleven tumor cell lines with gemcitabine and ubenimex as positive control ( $\text{IC}_{50}$  in  $\mu\text{M}$ )<sup>a</sup>

Cell lines	<b>BC-A1</b>	Gemcitabine (GEM)	Ubenimex (Ube)	GEM + Ube (1:1)
K562	$0.13 \pm 0.03$	$0.11 \pm 0.01$	>500	ND <sup>b</sup>
MDA-MB-231	$1.56 \pm 0.33$	$1.67 \pm 0.33$	>500	ND <sup>b</sup>
Hela	$5.48 \pm 0.39$	$2.74 \pm 0.09$	>500	ND <sup>b</sup>
ES-2	$0.28 \pm 0.12$	$0.53 \pm 0.15$	>500	ND <sup>b</sup>
3AO	$9.73 \pm 2.39$	$5.73 \pm 0.59$	>500	ND <sup>b</sup>
HEL	$0.61 \pm 0.05$	$0.48 \pm 0.05$	>500	ND <sup>b</sup>
A549	$0.66 \pm 0.05$	$0.26 \pm 0.02$	>500	ND <sup>b</sup>
PC-3	$0.26 \pm 0.01$	$0.22 \pm 0.04$	>500	ND <sup>b</sup>
U266	$0.26 \pm 0.09$	$0.22 \pm 0.14$	>500	ND <sup>b</sup>
U937	$0.08 \pm 0.01$	$0.07 \pm 0.01$	$142.63 \pm 17.46$	ND <sup>b</sup>
PLC/PRF/5	$1.41 \pm 0.45$	$1.53 \pm 0.42$	>500	ND <sup>b</sup>
KG1	$0.82 \pm 0.09$	$0.86 \pm 0.06$	>500	$1.01 \pm 0.12$

<sup>a</sup> Assays were performed in replicate ( $n \geq 2$ ); data are shown as mean  $\pm$  SD.

<sup>b</sup> Not determined.

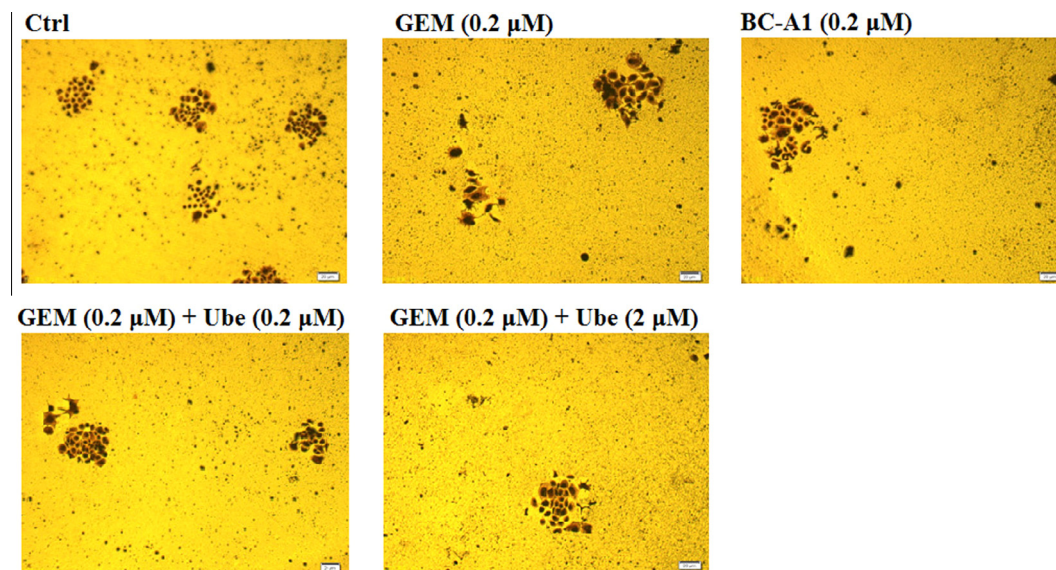


**Figure 3.** Colony formation by PLC/PRF/5 cells observed under an inverted microscope. Gemcitabine was used as a positive control. PLC/PRF/5 cells were stained with Giemsa after treatment with drugs for two consecutive weeks, and images were captured using an inverted microscope.

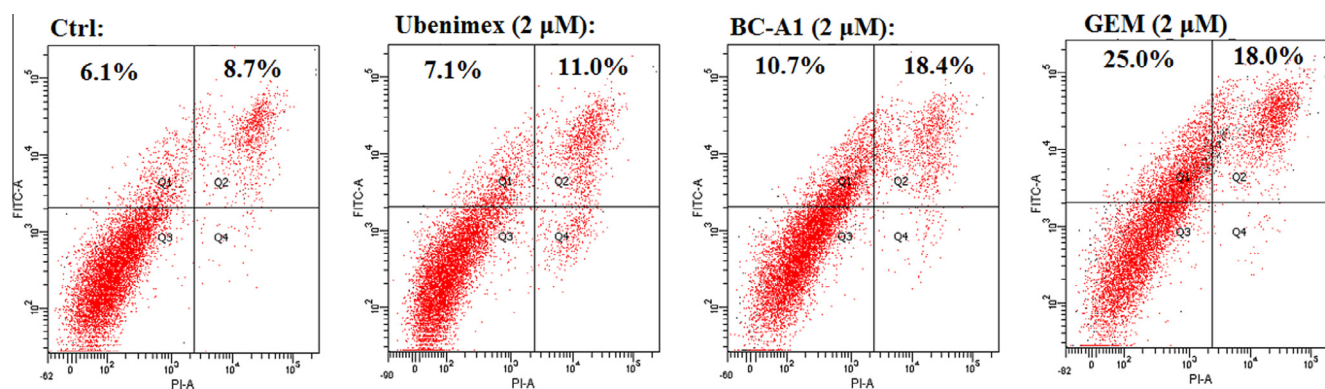


**Figure 4.** Induction of apoptosis at 48 h by compounds **BC-A1**, gemcitabine (positive control) and ubenimex (positive control), in PLC/PRF/5 cells.

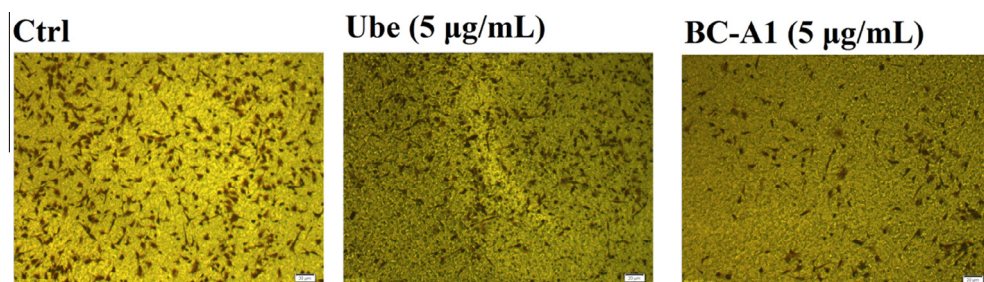


**Figure 5.** **BC-A1** inhibited ES-2 cells invasion in a transwell assay. Ubenimex was used as a positive control representative images indicate the inhibition of migration.

**BC-A1** was completely cleaved to their parent compounds ubenimex and gemcitabine within 120 min of incubations at 37 °C (Fig. 7). This is consistent with our initial design rationale.

### 3.7. In vivo antitumor activity assay

Due to the potent *in vitro* antiproliferative activity of **BC-A1**, *in vivo* antitumor study of **BC-A1** was investigated using H22 (mice hepatoma cell line) tumor transplant model in Kunming mice. In this experiment, the transplanted mice were randomly divided

into three groups. The mice were treated with an oral administration of PBS, single intraperitoneal administration of 25 mg/kg (0.084 mmol/kg) of gemcitabine, or oral administration of 25 mg/kg (0.042 mmol/kg) of **BC-A1**. The mice were treated with the test compounds at the specified dose every 4 days for a total of 4 doses (Q4D × 4). The results showed that compound **BC-A1** displayed potent oral antitumor activity, which is comparable with gemcitabine at the dosage of 25 mg/kg (Fig. 8a and b). It is worth noting that at the same dosage of 25 mg/kg, the mol concentration of gemcitabine in **BC-A1** (0.042 mmol/kg) is half of the mol

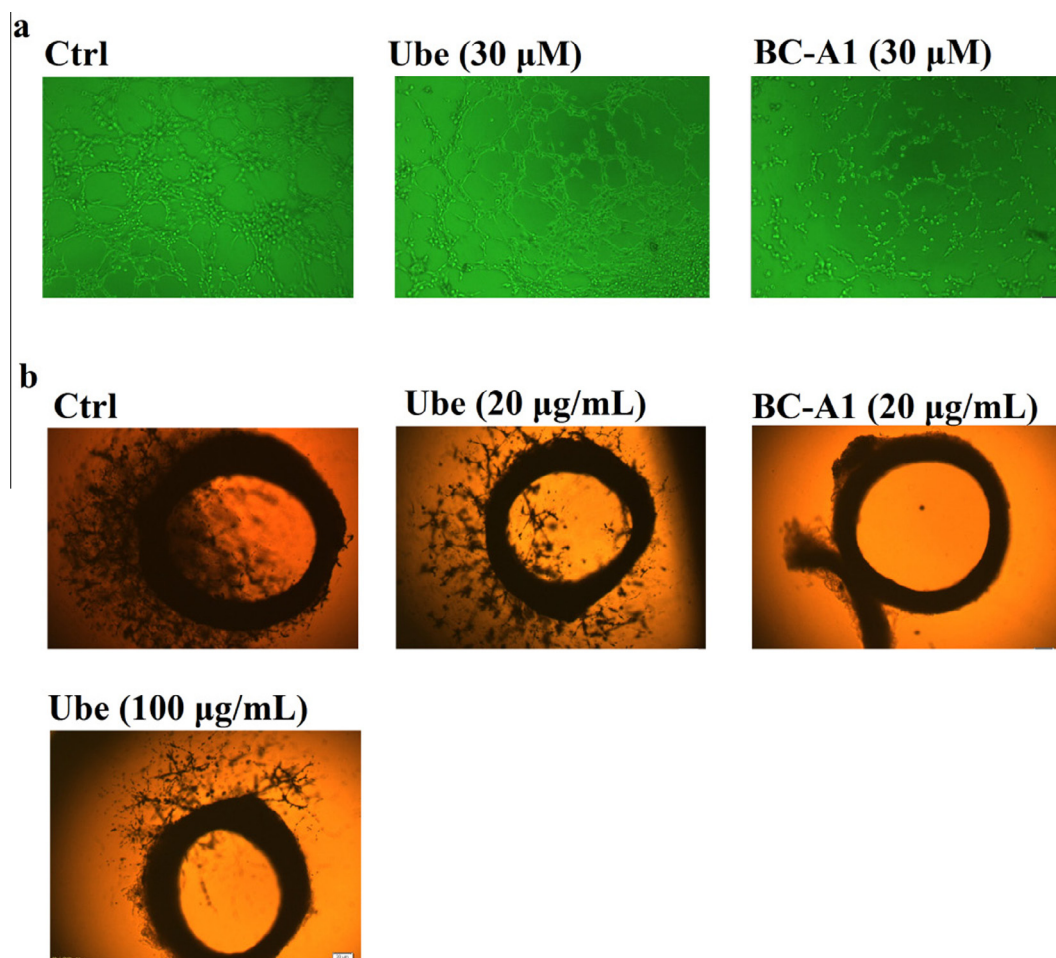


**Figure 6.** (a). Representative images of the tube formation assay depicting the formation of a HUVEC capillary-like tubular network by treatment with synthesized compound **BC-A1**. (b). Representative images of rat aortic rings treated with compound **BC-A1**, gemcitabine and ubenimex (positive control). The scale bar indicates 200 μm of length.

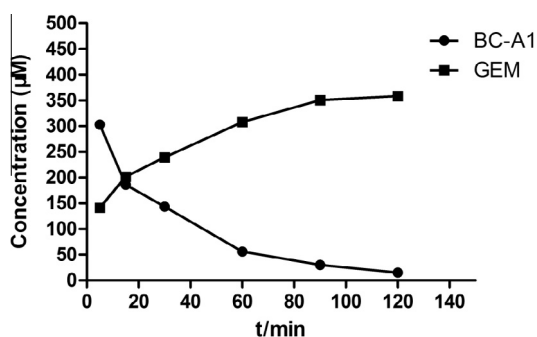


**Figure 7.** Stability of compound **BC-A1** in human plasma. Points of **BC-A1** were achieved after 5, 15, 30, 60, 90, 120 min.

concentration of gemcitabine (0.084 mmol/kg), which means the toxicity of **BC-A1** may decrease. Considering gemcitabine can not be orally administrated due to its toxicity<sup>35</sup>, our result suggests that **BC-A1** can be developed as an orally active prodrug of gemcitabine with less toxicity.

Encouraged by the potent oral antitumor activity of **BC-A1** in mouse hepatoma (H22) tumor transplant model, we further tested the effect of **BC-A1** in a human hepatoma (PLC/PRF/5) xenograft model. As shown in Figures 9 and 10, the antitumor potency of **BC-A1** (T/C = 51%) was similar to that of gemcitabine (T/C = 54%). Moreover, the in vivo antihepatoma activity of **BC-A1** was further

confirmed by another human hepatoma (HepG-2) xenograft model (Figs. 11 and 12).

#### 4. Conclusions

In summary, a mutual prodrug of gemcitabine and ubenimex was designed and synthesized. The in vitro pharmacology study on **BC-A1** showed that **BC-A1** displayed modest inhibition toward CD13, and inhibited the proliferation of representative cancer cell lines. The preliminary stability test of **BC-A1** revealed that it could release gemcitabine and ubenimex in human plasma. Meanwhile, the anti-tumor results indicated that **BC-A1** displayed potent oral antitumor activity, which is comparable with the positive control gemcitabine at the same dosage. Our comprehensive in vitro and in vivo antitumor activity evaluation supported further research and development of **BC-A1** as a promising mutual prodrug of gemcitabine and ubenimex. These results may also help us to develop novel orally active prodrug of gemcitabine. Evaluation of its pharmacokinetics in vivo is currently underway in our laboratory.

#### 5. Experimental section

##### 5.1. Chemistry

Starting materials, reagents, and solvents were obtained from commercial suppliers and used without further purification unless otherwise indicated. All reactions were monitored via thin layer

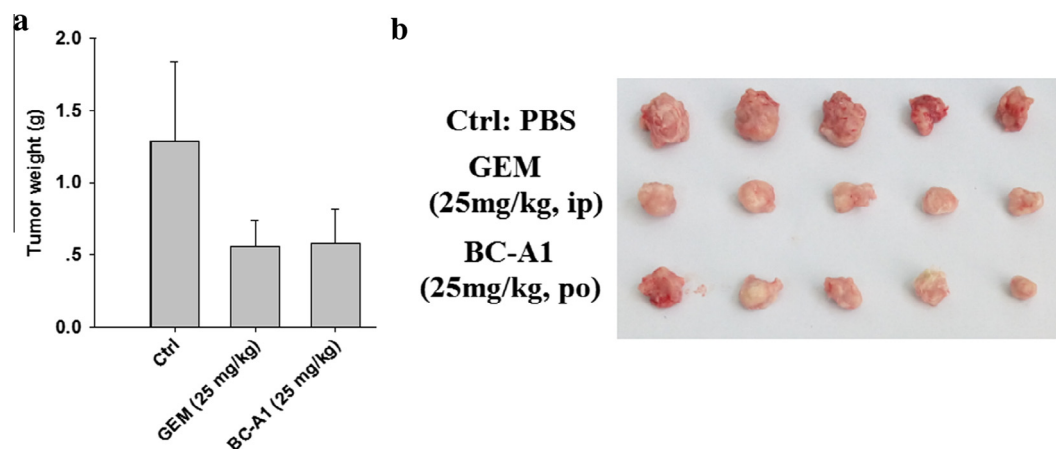


**Figure 8.** Antitumor effect of BC-A1 as tested using tumor-bearing Kunming mice with gemcitabine GEM (25 mg/kg/d) as a positive control. (a) Weights of tumors in different groups. (b) Photographs of tumors obtained from the tumor-bearing mice.

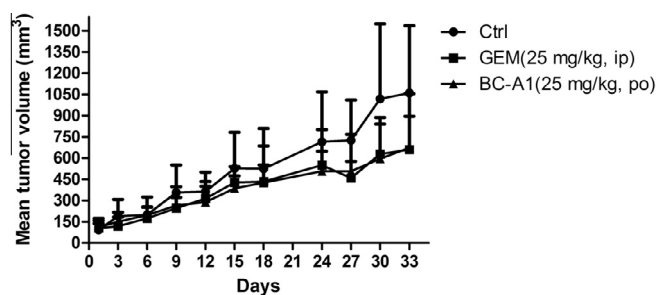


**Figure 9.** Growth curve of implanted PLC/PRF/5 xenograft in nude mice.

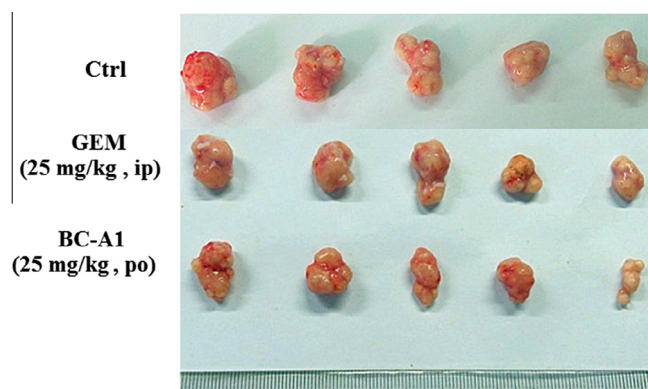


**Figure 10.** Picture of dissected PLC/PRF/5 tumor tissues.

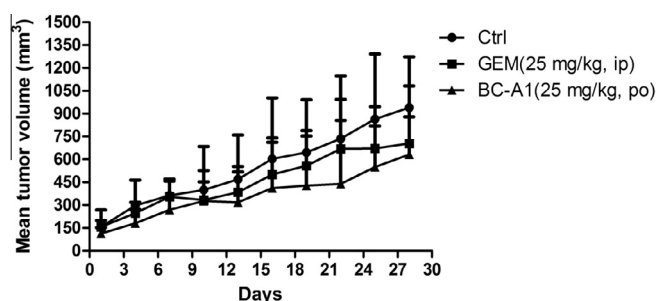


**Figure 11.** Growth curve of implanted HepG2 xenograft in nude mice.

chromatography (TLC) (0.25 mm silica gel plates (60GF-254)). UV light and ninhydrin were used to visualize the spots. Silica gel was used for column chromatography purification.  $^1\text{H}$  NMR spectra were routinely recorded on a Bruker DRX spectrometer at 400 MHz,  $\delta$  in parts per million and  $J$  in hertz, using Tetramethylsilane (TMS) as an internal standard. High-resolution mass spectrometry was performed by Shandong Analysis and Test Center in Ji'nan, China. ESI-MS spectra were recorded on an API 4000 spectrometer. Melting points were determined uncorrected on an electrothermal melting point apparatus. The purity of target compound was determined by HPLC using an ODS HYPERSIL column (5  $\mu\text{m}$ , 4.6 mm  $\times$  250 mm) with UV detection (249 nm) (22% acetonitrile/78% water (containing 0.1% triethylamine and 0.15% trifluoroacetic acid) over 30 min) to be 95%.

#### 5.1.1. (3S,4R)-4-((*tert*-Butoxycarbonyl)amino)-3-hydroxy-2-oxo-5-phenylpentanoic acid (**11**)

**10** (19.5 g, 100 mmol) was dissolved in 1 N NaOH solution (200 mL). The mixture was stirred under ice bath.  $(\text{Boc})_2\text{O}$  (26.2 g, 120 mmol) dissolved in 120 mL of THF was added into the solution. After 2 h, the ice bath was removed, and the mixture was stirred for another 24 h. After removing THF under vacuum, the solution was acidified to pH3 with 1 N HCl solution. The solution was washed with 30 mL of acetic ether for 3 times. The organic layer was collected and dried with anhydrous sodium sulfate over night. After evaporating the solvent, the residue was dried under vacuum to get white solid **2** (25.3 g, yield: 86%). mp: 105–106 °C.  $^1\text{H}$  NMR (400 MHz  $\text{DMSO-}d_6$ ):  $\delta$  1.21–1.52 (m, 9H), 2.94–2.96 (m, 2H), 3.92–4.22 (m, 2H), 6.63 (d,  $J = 6.0$  Hz, 1H), 7.23–7.30 (m, 5H). ESI-MS  $m/z$ : 296.6 ( $\text{M}+\text{H}$ ) $^+$ .

#### 5.1.2. (S)-Benzyl-2-((2S,3R)-3-((*tert*-butoxycarbonyl)amino)-2-hydroxy-4-phenylbutanamide)-4-methyl-pentanoate (**12**)

**11** (6 g, 20.3 mmol) and HOBT (3 g, 22.3 mmol) were dissolved in dry DCM (200 mL) under ice bath followed by the addition of EDCI (4.5 g, 22.3 mmol) and stirring for 30 min at room temperature. *l*-Leucine benzyl ester toluene-4-sulfonate (8.5 g, 22.3 mmol) and TEA (3.1 mL) were added into the solution directly. The mixture was stirred for 5 h at room temperature. The DCM solution was washed with 1 N HCl, saturated  $\text{NaHCO}_3$  and brine for 3 times, dried over anhydrous sodium sulfate and evaporated under vacuum. The crude product was purified by recrystallization with EtOAc and petroleum ether to achieve a white pure solid **12** (4.8 g, yield: 47.5%). mp: 148–150 °C.  $^1\text{H}$  NMR (400 MHz  $\text{DMSO-}d_6$ ):  $\delta$  0.78–0.87 (m, 6H), 1.16–1.28 (m, 9H), 1.45–1.52 (m, 1H),



Figure 12. Picture of dissected HepG2 tumor tissues.

1.57–1.75 (m, 2H), 2.62–2.67 (m, 1H), 2.76–2.82 (m, 1H), 3.84–3.95 (m, 2H), 4.39–4.45 (m, 1H), 5.11 (s, 2H), 6.00 (d,  $J = 6.6$  Hz, 1H), 6.16 (d,  $J = 9.3$  Hz, 1H), 7.16–7.27 (m, 3H), 7.29–7.38 (m, 7H), 8.02 (d,  $J = 8.5$  Hz, 1H). ESI-MS  $m/z$ : 499.6 (M+H)<sup>+</sup>.

### 5.1.3. (S)-2-((2S,3R)-3-((tert-Butoxycarbonyl)amino)-2-hydroxy-4-phenylbutan- amido)-4-methylpentanoic acid (13)

To a solution of **12** (4.9 g, 10.0 mmol) in methanol (200 mL), dry palladium-carbon (0.5 g) was added and the mixture was stirred under a hydrogen atmosphere overnight. The palladium-carbon was filtered off over celite, washed with methanol. After evaporating the solvent, the residue was dried under vacuum to get white solid **13** (3.8 g, yield: 92.0%). mp: 124–125 °C. <sup>1</sup>H NMR (400 MHz DMSO-*d*<sub>6</sub>):  $\delta$  0.81–0.88 (m, 6H), 1.15–1.29 (m, 9H), 1.44–1.50 (m, 1H), 1.58–1.67 (m, 2H), 2.65–2.67 (m, 1H), 2.77–2.82 (m, 1H), 3.83–3.92 (m, 2H), 4.27–4.32 (m, 1H), 6.04 (d,  $J = 6.2$  Hz, 1H), 6.16 (d,  $J = 9.2$  Hz, 1H), 7.18–7.29 (m, 5H), 7.78 (d,  $J = 8.6$  Hz, 1H), 12.68 (s, 1H). ESI-MS  $m/z$ : 409.6 (M+H)<sup>+</sup>.

### 5.1.4. 4-Amino-1-((2R,4R,5R)-4-((tert-butyldimethylsilyl)oxy)-5-(((tertbutyldimethylsilyl)-oxy)methyl)-3,3-difluorotetrahydrofuran-2-yl)pyrimidin-2(1H)-one (15)

A solution of **14** (3.0 g, 10.0 mmol), *N*-methylimidazole (5.0 g, 30.0 mmol), and iodine (7.6 g, 30.0 mmol) were dissolved in dry tetrahydrofuran and pyridine (ratio 10:1, 100 mL). Subsequently, *t*-butyldimethylchlorosilane (TBSCl) (3.7 g, 25 mmol) was added. The reaction mixture was stirred at room temperature until complete disappearance of the starting material (TLC analysis). THF was evaporated with the residue being taken up in EtOAc (300 mL). The EtOAc solution was washed with saturated Na<sub>2</sub>S<sub>2</sub>O<sub>3</sub>, saturated NaHCO<sub>3</sub> and brine for 3 times, dried over anhydrous sodium sulfate over night, evaporated. The residue was purified by column chromatography, using DCM–MeOH (20:1) as the mobile phase, to obtain **15** as Pale yellow white solid (3.15 g, yield: 64%). mp: 118–120 °C. <sup>1</sup>H NMR (400 MHz DMSO-*d*<sub>6</sub>):  $\delta$  0.09–0.11 (m, 12H), 0.87–0.90 (m, 18H), 3.76–3.79 (m, 1H), 3.88–3.96 (m, 2H), 4.27–4.36 (m, 1H), 5.79 (d,  $J = 7.5$  Hz, 1H), 6.15–6.19 (m, 1H), 7.44 (d,  $J = 7.1$  Hz, 2H), 7.55 (d,  $J = 7.5$  Hz, 1H). ESI-MS  $m/z$ : 490.7 (M–H)<sup>–</sup>.

### 5.1.5. tert-Butyl-((2R,3S)-4-(((S)-1-(((1-((2R,4R,5R)-4-((tert-butyldimethylsilyl)oxy)-5-(((tert-butyldimethylsilyl)oxy)methyl)-3,3-difluorotetrahydrofuran-2-yl)-2-oxo-1,2-dihydropyrimidin-4-yl)amino)-4-methyl-1-oxopentan-2-yl)amino)-3-hydroxy-4-oxo-1-phenyl-butan-2-yl)carbamate (7)

**13** (4.1 g, 10.1 mmol) and HOBT (1.6 g, 12.2 mmol) were dissolved dry DCM (200 mL) under ice bath followed by the addition of EDCI (2.3 g, 12.2 mmol) and stirring for 30 min at room temperature. **15** (5.5 g, 11.1 mmol) and TEA (2.1 mL) were added into the solution directly. The mixture was stirred for 5 h at room temperature. The DCM solution was washed with 1 N aqueous citric acid, saturated NaHCO<sub>3</sub> and brine for 3 times, dried over anhydrous sodium sulfate and evaporated under vacuum. The residue was

purified by column chromatography, using PE–EtOAc (4:1) as the mobile phase, to obtain **7** as white solid (3.15 g, yield: 35%). mp: 108–110 °C, ESI-MS  $m/z$ : 882.8 (M+H)<sup>+</sup>.

### 5.1.6. tert-Butyl-((2R,3S)-4-(((S)-1-(((1-((2R,4R,5R)-3,3-difluoro-4-hydroxy-5-(hydr-oxymethyl)tetrahydrofuran-2-yl)-2-oxo-1,2-dihydropyrimidin-4-yl)amino)-4-methyl-1-oxopentan-2-yl)amino)-3-hydroxy-4-oxo-1-phenylbutan-2-yl)carbamate (17)

**7** (0.9 g, 1 mmol) was reacted with tetrabutylammonium fluoride (TBAF; 1 M in THF, 1.7 mL, 1.7 mmol) in 20 mL of THF for 2 h at room temperature. THF was evaporated under vacuum; the crude product was dissolved with EtOAc, washed by 1 N aqueous citric acid, saturated NaHCO<sub>3</sub> and brine for 3 times, dried over anhydrous sodium sulfate over night and the solvent was evaporated under vacuum. The crude product was purified via flash chromatography to afford the compound **17** (0.42 g, yield: 65%). mp: 196–197 °C. <sup>1</sup>H NMR (400 MHz DMSO-*d*<sub>6</sub>): 0.84–0.90 (m, 6H), 1.15–1.28 (m, 9H), 1.44–1.50 (m, 1H), 1.62–1.68 (m, 2H), 2.63–2.68 (m, 1H), 2.77–2.82 (m, 1H), 3.33–3.70 (m, 1H), 3.79–3.96 (m, 4H), 4.13–4.23 (m, 1H), 4.54–4.59 (m, 1H), 5.32 (t,  $J = 5.4$  Hz, 1H), 6.05 (d,  $J = 6.4$  Hz, 1H), 6.15–6.19 (m, 2H), 6.33 (d,  $J = 6.5$  Hz, 1H), 7.16–7.29 (m, 6H), 8.07–8.09 (m, 1H), 8.28 (d,  $J = 7.6$  Hz, 1H), 11.17 (s, 1H). HRMS (AP-ESI)  $m/z$  Calcd for C<sub>30</sub>H<sub>41</sub>F<sub>2</sub>N<sub>5</sub>O<sub>9</sub>, [M+H]<sup>+</sup> 654.2965. Found: 654.2968.

### 5.1.7. (S)-2-((2S,3R)-3-Amino-2-hydroxy-4-phenylbutanamido)-N-((1-((2R,4R,5R)-3,3-difluoro-4-hydroxy-5-(hydroxymethyl)tetrahydrofuran-2-yl)-2-oxo-1,2-dihydro-pyrimidin-4-yl)-4-methylpentanamide hydrochloride (9, BC-A1)

**17** (0.65 g, 1.0 mmol) was dissolved in saturated chloride hydrogen in dry ethyl acetate (40 mL). The mixture was stirred at room temperature for 2 h. The filtered precipitate was washed by diethyl ether to give the compound **9** (BC-A1), a white solid powder (0.43 g, yield: 91%). mp: 156–158 °C, <sup>1</sup>H NMR (400 MHz DMSO-*d*<sub>6</sub>): 0.83–0.92 (m, 6H), 1.50–1.70 (m, 3H), 2.89–2.98 (m, 2H), 3.53–3.67 (m, 2H), 3.79–3.82 (m, 1H), 3.89–3.91 (m, 1H), 4.01–4.06 (m, 1H), 4.10–4.35 (m, 1H), 4.41–4.51 (m, 1H), 6.10–6.23 (m, 1H), 7.20–7.37 (m, 7H), 8.04–8.08 (m, 3H), 8.28–8.33 (m, 2H), 11.28 (s, 1H). HRMS (AP-ESI)  $m/z$  Calcd for C<sub>25</sub>H<sub>33</sub>F<sub>2</sub>N<sub>5</sub>O<sub>7</sub>, [M+H]<sup>+</sup> 554.2421. Found: 554.2429. Retention time: 13.6 min, eluted with 22% acetonitrile/78% water (containing 0.1% triethylamine and 0.15% trifluoroacetic acid).

## 5.2. CD13 inhibition assay

The inhibitory activity of target compound toward CD13 was determined by using microsomal aminopeptidase from porcine kidney microsomes (Sigma) as the enzyme in 50 mM PBS, pH 7.2 at 37 °C. *L*-Leucine-*p*-nitroanilide was used as substrate. Briefly, the CD13 solution was added to tested compound solutions at various concentrations and incubated at 37 °C for 5 min. Then, the substrate was added and the mixture was incubated for another 30 min at 37 °C. Finally, the hydrolysis of the substrate was measured by following the change in the absorbance measured at 405 nm with a Micro-plate Reader (Thermo Fisher, Shanghai, China).

CD13 activity on the surface of ES-2 and PLC/PRF/5 cells was estimated by measuring the hydrolysis of substrate (*L*-leucine-*p*-nitro-anilide). A cell suspension (2.5 × 10<sup>6</sup>/mL) in 1 × PBS buffer was added to a 96-well plate (70 μL) containing various concentrations of test compounds. Then, the solution of substrate was added to each well and the mixture was incubated for 1 h at 37 °C. CD13 activity was estimated by measuring the absorbance at 405 nm as described above.

### 5.3. Cell proliferation analysis

All cell lines were maintained in RPMI1640 medium containing 10% FBS at 37 °C in a 5% CO<sub>2</sub> humidified incubator. Cell proliferation assay was determined by the MTT method. Briefly, cells were passaged the day before dosing into a 96-well cell plate, allowed to grow for 12 h and then treated with different concentrations of compound sample for 48 h. A 0.5% MTT solution was added to each well. After incubation for another 4 h, formazan formed from MTT was extracted by adding 150  $\mu$ L of DMSO rocking for 15 min. Absorbance was then determined using an ELISA reader at 570 nm. The IC<sub>50</sub> values were calculated according to the inhibition ratios.

### 5.4. Colony formation assay

For the colony formation assay, PLC/PRF/5 cells ( $0.5 \times 10^3$ /well) were seeded in 6-well plates. After 12 h, cells were exposed to **BC-A1**, GEM, and a combination of the GEM and ubenimex (1:1) at 37 °C. After two weeks, cells were fixed with fresh 4% paraformaldehyde at room temperature for 15 min and stained with giemsa. Cell images were captured using an inverted microscope (magnification  $\times 4$ , Olympus, Beijing, China). A minimum of 50 viable cells were scored as a colony.

### 5.5. Flow cytometry

Flow cytometry was used to evaluate the cell apoptosis. PLC/PRF/5 cells seeded on 6-well plates ( $2 \times 10^5$  per well) were treated with test compounds for 48 h. Subsequently, cells were harvested, washed twice in cold PBS, centrifuged, and resuspended in  $1 \times$  annexin-binding buffer according to the instruction of the apoptosis kit. Annexin V-FITC and propidium iodide were added to each tube and incubated for 15 min in the dark. The stained cells were analyzed by flow cytometry. The results were compared with control groups.

### 5.6. In vitro HUVEC tuber formation assay<sup>39</sup>

The 96-well microplates were coated with 100  $\mu$ L of Matrigel (BD Biosciences, NJ) and allowed to gel for 30 min at 37 °C and 5% CO<sub>2</sub>. Then, HUVECs were seeded at a density of 40,000 cells per well in M199 (5% FBS) containing the test compounds and incubated at 37 °C, 5% CO<sub>2</sub> for 6 h. The morphological changes of the cells and the tubular structure formation of HUVECs were observed under a phase-contrast microscope and photographed at  $200\times$  magnification.

### 5.7. Rat thoracic aorta rings (TARs) assay

The 96-well tissue culture plates were coated with 100  $\mu$ L of Matrigel (BD Biosciences, NJ) and allowed to gel for 30 min at 37 °C, 5% CO<sub>2</sub>. Then, the thoracic aortas were excised from 8- to 10-week-old male Wistar rats. After careful removal of fibroadipose tissues, the aortas were cut into 1-mm-long cross-sections, placed on Matrigel-coated wells, and covered with an additional 100  $\mu$ L of Matrigel. After the second layer of Matrigel set, the rings were incubated at 37 °C and 5% CO<sub>2</sub> for 30 min. Aorta rings were treated every other day with test compounds for 9 days and photographed on the 10th day at  $200\times$  magnification. Experiments were repeated three times using aortas from four different rats.

### 5.8. Invasion assay

Transwell filters were coated with matrigel (BD Biosciences, NJ) on the upper surface of a polycarbonic membrane and allowed to

gel for 30 min at 37 °C, 5% CO<sub>2</sub>. Harvested cells in serum-free RPMI-1640 (400  $\mu$ L) were added into the upper compartment of the chamber. Subsequently, 100  $\mu$ L of test compounds were added into the upper compartment of the chamber. 750  $\mu$ L of conditioned medium, which derived from ES-2 cells, was placed in the bottom compartment of the chamber. After 24 h incubation at 37 °C and 5% CO<sub>2</sub>, the medium was removed from the upper chamber. Cotton swab was used to scrape off the non-invaded cells on the upper side of the chamber. The cells, which had migrated from the matrigel into the pores of the inserted filter, were stained with crystal violet solution.

### 5.9. Stability of representative compound in human plasma

Preparation of human plasma was conducted as previously described.<sup>40</sup> Human plasma added to the stock solution of **BC-A1** (4 mg/mL in methanol) and incubated at 37 °C for 24 h. At scheduled times sample aliquots were collected and the enzymatic reaction was quenched by adding acetonitrile. Human Plasma samples underwent extraction using 300  $\mu$ L acetonitrile and 300  $\mu$ L water. The samples were filtered (0.22  $\mu$ m) after shocking 30 s and centrifugation at 12,000 rpm for 10 min. Analytical HPLC was performed on Agilent 1200 HPLC instrument using a Alltima C<sub>18</sub> column (5  $\mu$ m, 4.6 mm  $\times$  250 mm), compounds were eluted with 22% acetonitrile/78% water (containing 0.1% triethylamine and 0.15% trifluoroacetic acid) over 15 min. The absorbance was measured at 249 nm, the flow rate was 1 mL/min and the quantity of injection was 20  $\mu$ M.

### 5.10. In vivo tumor transplant models

All experiments involving in laboratory animals were performed the approval of the local ethics committee. In this experiment, to establish a solid tumor model, mice were inoculated subcutaneously with injections of  $1 \times 10^7$ /mL murine H22 cells (0.2 mL). When the tumor was approximately 0.2 cm<sup>3</sup> in size, the transplanted mice were randomly divided into treatment and control groups. The mice were treated with the test compounds at the specified dose for two weeks (every 4 days for a total of 4 doses (Q4D  $\times$  4)). After treatment, mice were sacrificed and dissected to weigh the tumor tissues and to examine the internal organ injury. The body weight was monitored regularly. The tumor inhibitory rate (%) was calculated as  $(1 - \text{average tumor weight/average tumor weight of PBS group}) \times 100\%$ .

### 5.11. In vivo human tumor xenograft models

In vivo tumor xenograft models were established as previously reported.<sup>41</sup> In Brief, two human liver tumor (PLC/PRF/5 and HepG2) cell lines were cultured in DMEM growth medium containing 10% FBS and maintained in a 5% CO<sub>2</sub> humidified incubator at 37 °C. For in vivo anti-tumor efficacy research, tumor cells were inoculated subcutaneously in the right flanks of female athymic nude mice (BALB/c-nu mice, 5–6 weeks old, Slac Laboratory Animal, Shanghai, China). When the tumor was approximately 100 mm<sup>3</sup> in size, the mice were randomized into treatment and control groups. The treatment groups received specified concentrations of compounds by oral administration or intravenous injection, and the blank control group received an equal volume of PBS solution. During treatment, the body weight was monitored regularly. After treatment, mice were sacrificed and dissected to weigh the tumor tissues and to examine the internal organ injury. The tumor inhibitory rate (%) was calculated as  $(1 - \text{average tumor weight of treatment group/average tumor weight of PBS group}) \times 100\%$ .

## Acknowledgments

This work was supported by National Natural Science Foundation of China (Grant Nos. 81373282, 21302111 and 81503108), National High-tech R&D Program of China, 863 Program (Grant No. 2014AA020523), and National Major Scientific and Technological Special Project for “Significant New Drugs Development” of China (Grant No. 2012ZX09103101-015), Major Project of Science and Technology of Shandong Province (2015ZDJS04001), Young Scholars Program of Shandong University (YSPSDU, Grant no. 2016WLJH33).

## References and notes

- Rawlings, N. D.; Barrett, A. J. *Nucleic Acids Res.* **1999**, *27*, 325.
- Luan, Y.; Xu, W. *Curr. Med. Chem.* **2007**, *14*, 639.
- Antczak, C.; De Meester, I.; Bauvois, B. J. *Biol. Regul. Homeost. Agents* **2001**, *15*, 130.
- Mina-Osorio, P. *Trends Mol. Med.* **2008**, *14*, 361.
- Fujii, H.; Nakajima, M.; Saiki, I.; Yoneda, J.; Azuma, I.; Tsuruo, T. *Clin. Exp. Metastasis* **1995**, *13*, 337.
- Rangel, R.; Sun, Y.; Guzman-Rojas, L.; Ozawa, M. G.; Sun, J.; Giordano, R. J.; Van Pelt, C. S.; Tinkey, P. T.; Behringer, R. R.; Sidman, R. L., et al. *Proc. Natl. Acad. Sci. U.S.A.* **2007**, *104*, 4588.
- Arap, W.; Pasqualini, R.; Ruoslahti, E. *Science* **1998**, *279*, 377.
- Pasqualini, R.; Koivunen, E.; Kain, R.; Lahdenranta, J.; Sakamoto, M.; Stryhn, A.; Ashmun, R. A.; Shapiro, L. H.; Arap, W.; Ruoslahti, E. *Cancer Res.* **2000**, *60*, 722.
- Haraguchi, N.; Ishii, H.; Mimori, K.; Tanaka, F.; Ohkuma, M.; Kim, H. M.; Akita, H.; Takiuchi, D.; Hatano, H.; Nagano, H., et al. *J. Clin. Invest.* **2010**, *120*, 3326.
- Guzman-Rojas, L.; Rangel, R.; Salameh, A.; Edwards, J. K.; Dondossola, E.; Kim, Y. G.; Saghatelian, A.; Giordano, R. J.; Kolonin, M. G.; Staquicini, F. I., et al. *Proc. Natl. Acad. Sci. U.S.A.* **2012**, *109*, 1637.
- Schorlemmer, H. U.; Bosslet, K.; Dickneite, G.; Luben, G.; Sedlacek, H. H. *Behring Inst. Mitt.* **1984**, 157.
- Ota, K.; Uzuka, Y. *Biotherapy* **1992**, *4*, 205.
- Ota, K.; Kurita, S.; Yamada, K.; Masaoka, T.; Uzuka, Y.; Ogawa, N. *Cancer Immunol. Immunother.* **1986**, *23*, 5.
- Carmichael, J.; Fink, U.; Russell, R. C.; Spittle, M. F.; Harris, A. L.; Spiessi, G.; Blatter, J. *Br. J. Cancer* **1996**, *73*, 101.
- Favaretto, A. *Ann. Oncol.* **2006**, *17*, v82.
- Mornex, F.; Girard, N. *Ann. Oncol.* **2006**, *17*, 1743.
- Burris, H. r.; Moore, M. J.; Andersen, J.; Green, M. R.; Rothenberg, M. L.; Modiano, M. R.; Cripps, M. C.; Portenoy, R. K.; Storniolo, A. M.; Tarassoff, P. J. *Clin. Oncol.* **1997**, *15*, 2403.
- Hilbig, A.; Oettle, H. *Expert Rev. Anticancer* **2008**, *8*, 511.
- Lorusso, D.; Di Stefano, A.; Fanfani, F.; Scambia, G. *Ann. Oncol.* **2006**, *17*, v188.
- Thigpen, T. In *Semin. Oncol.*; Elsevier, 2006; p 26.
- Dent, S.; Messersmith, H.; Trudeau, M. *Breast Cancer Res. Treat.* **2008**, *108*, 319.
- Karak, F. E.; Flechon, A. *Expert Opin. Pharmacol.* **2007**, *8*, 3251.
- Yardley, D. A. In *Semin. Oncol.*; Elsevier, 2005; p 14.
- Ozols, R. F. In *Semin. Oncol.*; Elsevier, 2005; p 4.
- Munhoz, R. R.; D'Angelo, S. P.; Gounder, M. M.; Keohan, M. L.; Chi, P.; Carvajal, R. D.; Singer, S.; Crago, A. M.; Landa, J.; Healey, J. H., et al. *Oncologist* **2015**, *20*, 1245.
- Ramanathan, R. K.; Goldstein, D.; Korn, R. L.; Arena, F.; Moore, M.; Siena, S.; Teixeira, L.; Taberner, J.; Van Laethem, J. L.; Liu, H., et al. *Ann. Oncol.* **2016**, *27*, 648.
- Storniolo, A. M.; Allerheiligen, S. R.; Pearce, H. L. *Semin. Oncol.* **1997**, *24*, S7.
- Veltkamp, S. A.; Jansen, R. S.; Callies, S.; Pluim, D.; Visseren-Grul, C. M.; Rosing, H.; Kloeker-Rhoades, S.; Andre, V. A.; Beijnen, J. H.; Slapak, C. A. *Clin. Cancer Res.* **2008**, *14*, 3477.
- Clarke, M. L.; Mackey, J. R.; Baldwin, S. A.; Young, J. D.; Cass, C. E. In *Clinically Relevant Resistance in Cancer Chemotherapy*; Springer, 2002; p 27.
- Bergman, A. M.; Pinedo, H. M.; Peters, G. J. *Update* **2002**, *5*, 19.
- Ueno, H.; Kiyosawa, K.; Kaniwa, N. *Br. J. Cancer* **2007**, *97*, 145.
- Mini, E.; Nobili, S.; Caciagli, B.; Landini, I.; Mazzei, T. *Ann. Oncol.* **2006**, *17*, v7.
- Moysan, E.; Bastiat, G.; Benoit, J.-P. *Mol. Pharm.* **2012**, *10*, 430.
- Slusarczyk, M.; Lopez, M. H.; Balzarini, J.; Mason, M.; Jiang, W. G.; Blagden, S.; Thompson, E.; Ghazaly, E.; McGuigan, C. J. *Med. Chem.* **2014**, *57*, 1531.
- Bender, D. M.; Bao, J.; Dantzig, A. H.; Diserod, W. D.; Law, K. L.; Magnus, N. A.; Peterson, J. A.; Perkins, E. J.; Pu, Y. J.; Reutzel-Edens, S. M., et al. *J. Med. Chem.* **2009**, *52*, 6958.
- Jiang, Y.; Li, X.; Hou, J.; Huang, Y.; Jia, Y.; Zou, M.; Zhang, J.; Wang, X.; Xu, W.; Zhang, Y. *Eur. J. Med. Chem.* **2016**, *121*, 649.
- Yoneda, J.; Saiki, I.; Fujii, H.; Abe, F.; Kojima, Y.; Azuma, I. *Clin. Exp. Metastasis* **1992**, *10*, 49.
- Aozuka, Y.; Koizumi, K.; Saitoh, Y.; Ueda, Y.; Sakurai, H.; Saiki, I. *Cancer Lett.* **2004**, *216*, 35.
- Xu, F.; Jia, Y.; Wen, Q.; Wang, X.; Zhang, L.; Zhang, Y.; Yang, K.; Xu, W. *Eur. J. Med. Chem.* **2013**, *64*, 377.
- Li, X.; Inks, E. S.; Li, X.; Hou, J.; Chou, C. J.; Zhang, J.; Jiang, Y.; Zhang, Y.; Xu, W. *J. Med. Chem.* **2014**, *57*, 3324.
- Zhang, Y.; Feng, J.; Jia, Y.; Wang, X.; Zhang, L.; Liu, C.; Fang, H.; Xu, W. *J. Med. Chem.* **2011**, *54*, 2823.